Research Article

Hepatoprotective effect of *Monotheca buxifolia* fruit against antitubercular drugs-induced hepatotoxicity in rats

Hepatoprotective effect of *Monotheca buxifolia* fruit against antitubercular drugs–induced hepatotoxicity in rats

Irfan Ullah[1], Jamshaid Ali Khan[1], Achyut Adhikari[2] and Muhammad Shahid[1]

[1]Department of Pharmacy, University of Peshawar, Peshawar, Pakistan; [2]HEJ Research Institute of Chemistry, International Centre for Chemical and Biological Sciences, University of Karachi, Karachi, Pakistan.

Abstract

The present study investigates the hepatoprotective potential of *Monotheca buxifolia* fruit hydro-ethanolic extract, against isoniazid- and rifampicin-induced hepatotoxicity in rats. Phytochemical investigations lead to the isolation of oleanolic acid and isoquercetin. Pretreatment with *M. buxifolia* extract at doses of 150 and 300 mg/kg for 21 days, restored the isoniazid- and rifampicin-induced elevation of serum levels of alanine aminotransferase ($p<0.001$), aspartate aminotransferase ($p<0.001$ and $p<0.05$), alkaline phosphatase ($p<0.001$), billirubin ($p<0.001$) and total proteins ($p<0.001$) as well as afforded significant protection against histopathological changes in the liver. From these results, it is conceivable that *M. buxifolia* exhibited selective protective effect against isoniazid- and rifampicin-induced hepatotoxicity, mediated through the presence of oleanolic acid and isoquercetin.

Introduction

Liver is the major organ of xenobiotic metabolism and detoxification, which makes it vulnerable to hepatotoxicity (Lee, 1993). Many drugs are hepatotoxic including antitubercular drugs i.e., isoniazid and rifampicin (Sheen et al., 2014). Oxidative stress, toxic metabolites production and induction of cytochrome P_{450} 2E1 are the culminating findings of isoniazid- and rifampicin-induced hepatotoxicity (Qader et al., 2014). Isoniazid and rifampicin are the first line drugs for treatment of tuberculosis. Therefore, strategies to make their safe clinical use are desperately required (Jehangir et al., 2010; Lian et al., 2013).

Monotheca buxifolia (Falc.) is a member of the genus *Monotheca* and belongs to family Sapotaceae. Several members of this family including *Bassia latifolia* (Sheikh et al., 2012), *Chrysophyllum albidum* (Adebayo et al., 2011), and *Madhuca longifolia* (Kumar et al., 2013) have been evaluated for hepatoprotective potential in various experimental models. Forlklorically, *M. buxifolia* fruit is used as hematinic, laxative, purgative, vermini-

cidal, antipyretic and in the management of gastro-urinary disorders (Marwat et al., 2011; Rehman et al., 2013; Shah et al., 2013; Ullah et al., 2010). *M. buxifolia* contains flavonoids, terpenoids, cardiac glycosides, anthraquinones, saponins, reducing sugars, tannins and polyphenolic compounds. Flavonoids and polyphenolic compounds possess potent antioxidant and hepatoprotective potential. Previously *in vitro* anti-oxidant potential of its fruit has been investigated (Jan et al., 2013).

Keeping in view the strong *in vitro* anti-oxidant potential of *M. buxifolia,* the current study further investigated the hyrdo-ethanolic extract of *M. buxifolia* fruit for its hepatoprotective potential against isoniazid- and rifampicin-induced hepatotoxicity in rats. The extract was also subjected to phytochemical isolation for its active compounds.

Materials and Methods

Plant material

Fruit of *M. buxifolia* was collected from the northern

areas of Pakistan in the month of August and authen-ticated by a taxonomist at the Department of Botany, University of Peshawar. A specimen was deposited in the herbarium of University of Peshawar for further reference (Bot. 20061-PUP).

Animals

Male Sprague Dawley rats (200 ± 20 g) were kept at standard conditions i.e. temperature 25 ± 2°C and 12 hours dark/light cycle throughout the experiment. The animals were fed with standard diet and tap water *ad libitum*.

Chemicals and drugs

Isoniazid and rifampicin were obtained from Schazo-Zaka while silymarin from Medicraft Pharmaceuticals. Formalin, xylene and normal phase silica were pur-chased from Merck, Germany. Serum diagnostic kits for biochemical assays were obtained from Chema Diagnos-tica (Italy). All solvents used were of analytical grade.

Preparation of extract

Fruit of *M. buxifolia* were collected and washed with distilled water to remove dust. Seeds were separated and fruit pulp was dried under shade in a well-venti-lated place at ambient temperature. The dried pulp was crushed to powder, subjected for extraction with hydro-ethanolic (30:70) solvent, shaken occasionally for 15 days and filtered through Whatman No. 1 filter paper. The solvent was evaporated under reduced pressure in a rotary evaporator (BUCHI Rotavapor R-200, Switzer-land) at 40°C (Video clip). The semisolid mass (*M. buxifolia* hydro-ethanolic extract) was kept in refrigera-tor.

Gross phytochemical investigation

M. buxifolia extract was screened for glycosides (Okun-lola et al., 2007), triterpenoids (Nayak and Pereira, 2006), tannins, flavonoids, saponins (Sofowora, 1996) and alkaloids (Nayak and Pereira, 2006; Oyedapo et al., 1999).

Isoniazid- and rifampicin-induced toxicity

Suspension of isoniazid and rifampicin were separately prepared and given to rats in dose of 50 mg/kg each for 21 days via oral gavage tube (Pal et al., 2006).

Experimental design

Animals were divided into five groups (n = 6) in follow-ing manner: Group 1: Saline as control, Group 2: Isoniazid plus rifampicin 50 mg/kg each, Group 3: *M. buxifolia* extract (150 mg/kg) one hour before isoniazid plus rifampicin (50 mg/kg each), Group 4: *M. buxifolia* extract (300 mg/kg) one hour before isoniazid plus rifampicin (50 mg/kg each), Group 5: (silymarin 100 mg/kg one hour before isoniazid plus rifampicin (50 mg/kg each).

Blood collection and serum preservation

At the end of experiment, animals were anesthetized with ketamine (i.p, 100 mg/kg). Blood was collected through cardiac puncture (Video clip) and immediately transferred to evacuated gel and clot activator centrifuge tubes (AST Diagnostics). Serum was separated by centrifugation at 3,000 rpm for 15 min (Centurion Scientific LTD, UK).

Biochemical assays

Serum was assayed for alanine aminotransferase (ALT), aspartate aminotransferase (AST), alkaline phosphatase (ALP), billirubin and total proteins (TP) according to the standard diagnostic kits protocol supplied by the manufacturer. The analysis was performed using double beam UV/Visible spectrometer (Lambda 25, Perkin Elmer, USA).

Histology

After 21 days of treatment, liver of each animal was excised and fixed in 10% neutrally buffered formalin for 48 hours. The tissues were dehydrated in graded ethanol solutions (50, 70, 80, 90, two changes each of 100%), cleared in two changes each of 100% xylene, infiltrated and embedded in paraffin wax. Tissue blocks were sectioned at 4 µm through a rotary microtome (SLEE Mainz CUT 5062, Germany), stained with Harris hematoxylin and eosin for microscopic observation (Labomed Lx400 with digital camera iVu 3100, USA). Histopathological changes were scored as none (–), mild (+), moderate (++), or severe (+++) damage.

Isolation and structure elucidation of compounds

M. buxifolia extract (2.304 kg) was mixed with 2.5 L distilled water and soaked overnight, extracted thrice with 5 L each of *n*-hexanes, chloroform, ethyl-acetate, and *n*-butanol to get *n*-hexane soluble (56 g), chloro-form soluble (57.7 g), ethyl acetate soluble (34.9 g) and *n*-butanol soluble (54.5 g) fractions respectively. Ethyl-acetate fraction (30 g) was subjected to vacuum liquid chromatography on normal phase silica gel and eluted using hexane, hexane-ethyl acetate, ethyl acetate, ethyla cetate-methanol and methanol with increasing polarity to yield 18 fractions (Fr. 1-18). Compound 1 (13 mg) was obtained from fraction 2 (1.2 g) through repeated column chromatography using hexanes-ethylacetate (9:1–8:2) while fraction 15 (1.4 g) was re-chromato-graphed on silica gel column using ethyl acetate-hexanes (8:2) to get compound 2 (15 mg). Purity of the compounds was assessed using TLC followed by spraying with ceric sulfate and heating. Structures were elucidated using various techniques such as ^{1}H-NMR, ^{13}C-NMR, 2D-NMR, EI-MS, FAB-MS, UV, and IR. All the data of the compounds were unambiguously matched with reported data from literature (Eldahshan, 2011; Seo et al., 1981).

Statistical analysis

Data were expressed as mean ± SD. Statistical analysis was done by one-way ANOVA followed by Tukey's *post hoc* test using Graph pad Prism 5 (Graph pad Software Inc. San Diego CA, USA).

Results

Phytochemical analysis

The gross phytochemical analysis of hexane extract of *M. buxifolia* showed the presence of glycosides, triterpenoids, saponins, tannins, flavonoids, reducing sugars and alkaloids (Table I). Further chromatographic separation along with different analytical techniques lead to isolation of 2 compounds, namely oleanolic acid as com-pound 1 and isoquercetin as compound 2.

Hepatoprotective activity

Biochemical analysis

As shown in Table II, treatment with isoniazid plus rifampicin (50 mg/kg each) for 21 days significantly raised ($p < 0.001$) the serum levels of ALT, AST, ALP, billirubin and TP as compared to saline treated animals. Pretreatment with *M. buxifolia* extract at 100 mg/kg (Group 3) restored the serum levels of ALT ($p < 0.001$), AST ($p < 0.05$), ALP ($p < 0.001$), billirubin ($p < 0.001$) and TP ($p < 0.001$) to normal as compared to isoniazid plus rifampicin alone treated animals (Group 2). Likewise, pretreatment with *M. buxifolia* extract at 300 mg/kg (Group 4) inhibited ($p < 0.001$) the isoniazid plus rifampicin induced elevation of serum ALT, AST, ALP,

billirubin and total protein. Moreover, highly signifi-cant restorative effect ($p < 0.001$) on serum levels of ALT, AST, ALP, billirubin and total proteins was noted in animals treated with silymarin at a dose of 100 mg/kg (Group 5) as compared to isoniazid plus rifampicin alone treated animals (Group 2).

Histopathological evaluation

After 21 days of treatment with isoniazid plus rifampicin, the central veins of the hepatic lobules were congested with red blood cells and their epithelium were disrupted (Figure 1). The hepatocytes were depleted of glycogen. The sinusoidal spaces were dilated and infiltrated by large number of lymphocytes. Increased numbers of focal aggregations of lymphocytes with necrotic hepatocytes were present around the central vein. Although the liver retained its characteristic lobular appearance, however the hepatocytes appeared necrotic and exhibited ballooning degeneration. Pretreatment with *M. buxifolia* extract (150 and 300 mg/kg) or silymarin (100 mg/kg) for 21 days provided significant protection against isoniazid plus rifampicin induced hepatotoxicity as no significant histopathological changes were observed in the liver (Figure 1; Table III).

Discussion

Drug induced hepatotoxicity occurs in a variety of mechanisms such as membrane disruption or cellular necrosis, which may be resulted from binding of drug or its metabolite to cellular proteins, making new adducts that serves as targets for immune system and activates immunological reactions (Ramaiah et al.,

Table I			
Gross phytochemical screening of *Monotheca buxifolia* (MBHE)			
Sample No.	Test	Observation	Result
1	500 mg of MBHE + 1 drop $FeCl_3$ + 1 mL glacial acetic acid +1 mL H_2SO_4 (conc.)	Appearance of brown ring color	Glycosides present
2	500 mg of MBHE + 0.5 mL Fehling A solution + 0.5 mL Fehling solutions + heat	Appearance of brick-red color	Reducing sugar present
3	300 mg MBHE + 3 mL $CHCl_3$ → warmed for 0.5 hour → 2 mL H_2SO_4 (conc.) added	Red color appearance in lower layer	Tri-terpenoids present
4	Aqueous aliquot of MBHE + $FeCl_3$ reagent	Appearance of greenish black color	Tannins present
5	500 mg MBHE + 5 mL dilute NH_3 solution → 2 mL H_2SO_4 (conc.) added	Appearance of Yellowish color	Flavonoids present
6	300 mg MBHE + H_2SO_4 → boil/cool→ add $CHCl_3$ →separate $CHCl_3$ layer + dilute NH_3 solution	Color change	Anthraquinone present
7	200 mg MBHE → boil + 5 mL distilled H_2O→ shudder vigorously→ froth formation + olive oil → shudder vigorously	Emulsion formation	Saponins present
8	1 drop of MBHE solution on TLC plate+ Dragen-dorff's reagent	Appearance of orange /red color	Alkaloids present

Table II

Effect of *Monotheca buxifolia* on isoniazid- and rifampicin-induced hepatotoxicity in rats

Treatment	ALT (U/L)	AST (U/L)	Billirubin (mg/dL)	Alkaline phosphatase (U/L)	Total protein (g/dL)
Group 1	48.3 ± 4.0	84.1 ± 7.7	0.4 ± 0.1	119 ± 5.0	7.8 ± 0.1
Group 2	140 ± 6.2[a]	131 ± 6.1[a]	1.2 ± 0.1[a]	184 ± 7.6[a]	3.5 ± 0.2[a]
Group 3	114 ± 8.0[b]	115 ± 7.2[c]	0.9 ± 0.1[b]	120 ± 8.3[b]	5.7 ± 0.5[b]
Group 4	62.5 ± 5.5[b]	91.3 ± 7.1[b]	0.7 ± 0.2[b]	114 ± 7.0[b]	6.7 ± 0.3[b]
Group 5	54.3 ± 4.6[b]	85.5 ± 6.3[b]	0.4 ± 0.1[b]	118 ± 9.4[b]	7.4 ± 0.3[b]

Values are expressed as mean ± SD; ANOVA followed by Tukey's *post hoc* test; [a]p<0.001 compared to group 1, [b]p<0.001, [c]p<0.05 compared to Group 2 (n = 6)

2001). Other causes might be the inhibition of drug metabolism pathways. Interruption in the bile flow or disruption of filaments at sub-cellular level of bile duct causes abnormal or disturbed bile secretions, leading to jaundice and minimal cellular injury. Programmed cell death or apoptosis due to tissue necrosis factor or FAS pathways and inhibition of mitochondrial functions lead to accumulation of reactive oxygen species and subsequently lipid peroxidation and cell death (Girling, 1982).

Isoniazid and rifampicin are the first line antitubercular drugs and are used as standard hepatotoxic in various experiments. Administration of isoniazid and rifampicin causes changes in both morphology and cellular function of liver. In the current study, Sprague dawly rats were given isoniazid plus rifampicin (50 mg/kg per day orally for 21 days) to induce hepatotoxicity. Three folds rise in transaminases level in the serum of animals was a biochemical warning of hepatic injury. Isoniazid and rifampicin are potent
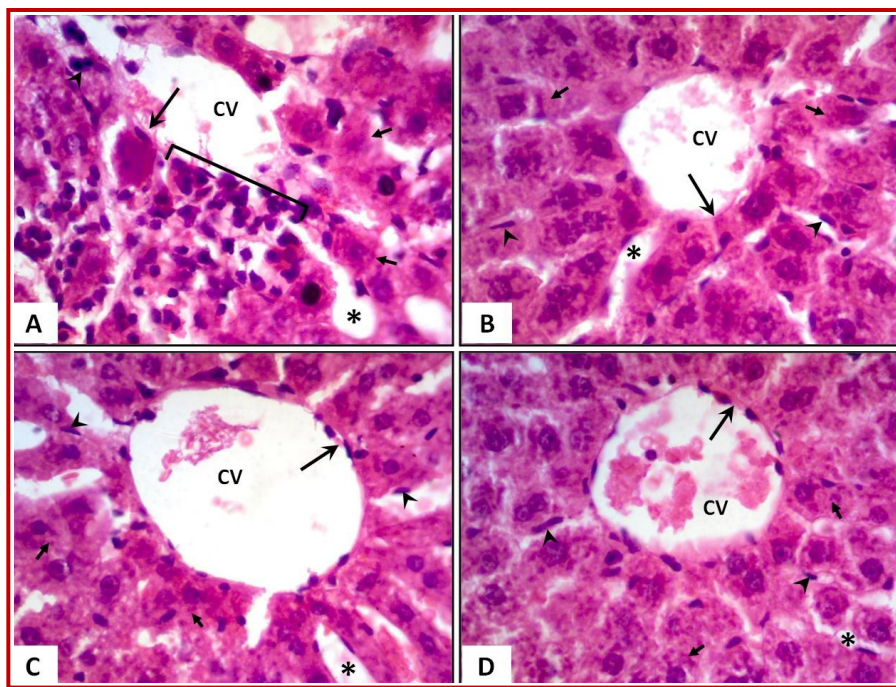

Figure 1: Histopathological evaluation of isoniazid plus rifampicin induced hepatotoxicity pretreated with *M. buxifolia* for 21 days (H and E; x400 original magnification). (A): Photomicrograph of a section of liver from a rat treated with isoniazid plus rifampicin showing congestion of the central vein (CV) with disruption of its endothelium (large arrow), dilatation of the sinusoidal spaces (asterisk), infiltration (arrow head) as well as aggregation (bar) of lymphocytes around the central vein and necrosis of hepatocytes (small arrows). Normal histology of central vein (CV) with intact endothelium (large arrow), hepatocytes (small arrows) and sinusoidal spaces (asterisk) lined by endothelial cells (arrow heads) were observed in groups of rats treated with (B): *M. buxifolia* (150 mg/kg) (C): *M. buxifolia* (300 mg/kg) and (D): silymarin (100 mg/kg) one hour before administration of isoniazid plus rifampicin

Table III					
Effect of *M. buxifolia* extract on isoniazid plus rifampicin induced hepatotoxicity after 21 days of treatment					
Histopathological findings	Group 1	Group 2	Group 3	Group 4	Group 5
Glycogen depletion	–	++	+	–	–
Congestion	+	+++	–	+	+
Endothelium disruption	–	+++	–	–	–
Sinusoidal dilatation	–	++	–	–	–
Hydropic degeneration	–	++	–	–	–
Cytolysis	–	+	–	–	–
Lymphocytic infiltration	–	++	+	–	–
Perivenular necrosis	–	++	–	–	–
Lymphoid aggregates in the portal tract	–	+++	–	–	–
(–) none; (+) mild; (++) moderate; (+++) severe damage					

hepatotoxic drugs shown by various studies but the exact mechanism of hepatotoxicity is still unclear. Isoniazid is converted to acetyl-isoniazid via hepatic N-acetyltransferase-2, which is then hydrolyzed to acetylhydrazine. Acetylhydrazine is oxidized by cytochrome P450 to form certain hepatotoxic intermediates. Hydrazine, either as direct (from isoniaizd) or indirect (from acetyl hydrazine) induces CYP2E1 (Poloyac et al., 2001). The best role of CYP2E1 is the production of reactive oxygen species which is a clear mechanism for the hepatotoxicity caused by isoniaizd (Yue et al., 2004). Rifampicin exaggerate the isoniazid hepatotoxicity possibly by increasing the production of hydrazine or inhibition of bile pathway (Dugasani et al., 2014; Rao et al., 2015). In this study, rifampicin and isoniazid significantly increased the serum levels of ALT, AST, ALP and billirubin while it decreased the level of TP. However, treatment with *M. buxifolia* extract at doses of 150 and 300 mg/kg significantly decreased the isoniazid and rifampicin induced elevated serum levels of ALT, AST, ALP, billirubin and total protein, and this protective effect was comparable to the standard hepatoprotective drug silymarin, thus proving the hepatoprotective effect of *M. buxifolia*. The biochemical investigation was corroborated by histopathological findings which showed that there are certain morphological changes which are typical of rifampicin and isoniazid induced hepatotoxicity. Treatment with *M. buxifolia* at both doses (150 and 300 mg/kg) significantly inhibited these morphological changes. These observations strongly supported the hepatoprotective potential of *M. buxifolia* fruit against isoniazid and rifampicin induced hepatotoxicity in rats.

M. buxifolia extract was fractioned and eluted through column chromatography. Two compounds were isolated which are characterized as isoquercetin and oleanolic acid. Isoquercetin is a potent anti-oxidant and is responsible for free radical scavenging activity while oleanolic acid is proved to regenerate glutathione and inhibit the induction of CYP2E1 (Delnavazi, 2015; Jeong, 1999; Yim et al., 2001). Due to the presence of

these compounds it might be suggested that the possible mechanism of *M. buxifolia* fruit for the hepatoprotective effect is the glutathione regeneration and reduction of oxidative stress by preventing the induction of CYP2E1 and scavenging free radicals.

Conclusion

The hydroethanolic extract of *M. buxifolia* fruit possessed potent hepatoprotective activity as demonstrated by significant amelioration of isoniazid- and rifampicin-induced biochemical and histopathological changes in liver. The significant hepatoprotective activity of *M. buxifolia* might be due to the presence of isoquercetin and oleanolic acid.

Ethical Issue

The experimental protocols for this study were approved by the ethical committee of the Department of Pharmacy, University of Peshawar, Pakistan (registration number: 04/EC-15/Pharm).

Conflict of Interest

Authors declare no conflict of interest

References

Adebayo AH, Abolaji AO, Kela R, Oluremi SO, Owolabi OO, Ogungbe OA. Hepatoprotective activity of *Chrysophyllum*

albidum against carbon tetrachloride induced hepatic damage in rats. Canadian J Pure app sci. 2011; 2: 1597-602.

Delnavazi M-rH A, Delazar A, Ajani Y, Tavakoli S, Yassa N. Phytochemical and anti-oxidant investigation of the aerial parts of *Dorema glabrum* Fisch. and CA Mey (2015 summer). Iranian J Pharm Res. 2015; 14: 12-24.

Dugasani SR, Saleem T, Sowjanya G, Gopinath C. Hepato-protective activity of methanolic extract of *Mussaenda philippica* (stems) against anti-tubercular drugs induced hepatotoxicity. Int J Pharmacol Res. 2014; 4: 199-202.

Eldahshan O. Isolation and structure elucidation of phenolic compounds of carob leaves grown in Egypt. Curr Res J Biol Sci. 2011; 3: 52-55.

Girling D. Adverse effects of antitubereulosis drugs. Drugs 1982; 23: 56-74.

Jan S, Khan MR, Rashid U, Bokhari J. Assessment of anti-oxidant potential, total phenolics and flavonoids of different solvent fractions of *Monotheca buxifolia* fruit. Osong Public Health Res Perspect. 2013; 4: 246-54.

Jehangir A, Nagi A, Shahzad M, Azam Z. The hepatopro-tective effect of *Cassia fistula* (amaltas) leaves in isoniazid and rifampicin induced hepatotoxicity in rodents. Biomedica 2010; 26: 25-29.

Jeong HG. Inhibition of cytochrome P450 2E1 expression by oleanolic acid: Hepatoprotective effects against carbon tetra-chloride-induced hepatic injury. Toxicol Lett. 1999; 105: 215-22.

Kumar A, Biswas K, Setty SR. Evaluation of the antioxidant and hepatoprotective activity of *Madhuca longifolia* (Koenig) leaves. Indian J Res Pharm Biotechnol. 2013; 1: 191-96.

Lee W. Drug-induced hepatotoxicity. Aliment Pharmacol Ther. 1993; 7: 477-85.

Lian Y, Zhao J, Xu P, Wang Y, Zhao J, Jia L, Fu Z, Jing L, Liu G, Peng S. Protective effects of metallothionein on isoniazid and rifampicin-induced hepatotoxicity in mice. PloS One. 2013; 8: e72058.

Marwat SK, Rehman F, Usman K, Khakwani A, Ghulam S, Anwar N, Sadiq M. Medico-ethnobotanical studies of edible wild fruit plants species from the flora of north western Pakistan (DI Khan district). J Med Plant Res. 2011; 5: 3679-86.

Nayak B, Pereira LMP. *Catharanthus roseus* flower extract has wound-healing activity in Sprague Dawley rats. BMC Complement Altern Med. 2006; 6: 41.

Okunlola A, Adewoyin BA, Odeku OA. Evaluation of pharmaceutical and microbial qualities of some herbal medicinal products in south-western Nigeria. Trop J Pharm Res. 2007; 6: 661-70.

Oyedapo O, Sab F, Olagunju J. Bioactivity of fresh leaves of *Lantana camara*. Biomed Lett. 1999; 59: 175-83.

Pal R, Vaiphei K, Sikander A, Singh K, Rana SV. Effect of garlic on isoniazid and rifampicin induced hepatic injury in rats. World J Gastroenterol. 2006; 12: 636-39.

Poloyac SM, Perez A, Scheff S, Blouin RA. Tissue-specific alterations in the 6-hydroxylation of chlorzoxazone following traumatic brain injury in the rat. Drug Metab Dispos. 2001; 29: 296-98.

Qader GI, Aziz R, Ahmed Z, Abdullah Z, Hussain SA. Protective effects of quercetin against isoniazid and rifampicin induced hepatotoxicity in rats. Am J Pharmacol Sci. 2014; 2: 56-60.

Ramaiah SK, Apte U, Mehendale HM. Cytochrome P4502E1 induction increases thioacetamide liver injury in diet restricted rats. Drug Metab Dispos. 2001; 29: 1088-95.

Rao CV, Singh A, Kumar GR, Gupta SS, Singh S, Rawat A. Hepatoprotective potential of *Ziziphus oenoplia* (L.) Mill roots against paracetamol induced hepatotoxicity in rats. Adv J Phytomed Clin Therap. 2015; 3: 064-78.

Rehman J, Khan IU, Farid S, Kamal S, Aslam N. Phytochemical screening and evaluation of *in-vitro* antioxidant potential of *Monotheca buxifolia*. E3 J Biotechnol Pharm Res. 2013; 4: 54-60.

Seo S, Tomita Y, Tori K. Biosynthesis of oleanene- and ursene-type triterpenes from [4-13C] mevalonolactone and sodium [1, 2-13C2] acetate in tissue cultures of *Isodon japonicus* Hara. J Am Chem Soc. 1981; 103: 2075-80.

Shah A, Marwat SK, Gohar F, Khan A, Bhatti KH, Amin M, Din NU, Ahmad M, Zafar M. Ethnobotanical study of medicinal plants of semi-tribal area of Makerwal and Gulla Khel (lying between Khyber Pakhtunkhwa and Punjab Provinces), Pakistan. Am J Plant Sci. 2013; 4: 98-116.

Sheen E, Huang RJ, Uribe LA, Nguyen MH. Isoniazid hepato-toxicity requiring liver transplantation. Digest Dis Sci. 2014; 59: 1370-74.

Sheikh RA, Babu DJM, Rao NV, Irene PR, More S, Turaskar A. Hepatoprotective activity of alcoholic and aqueous extracts of bark of *Bassia Latifolia* Roxb. against paracetamol induce hepatotoxicity in rats. Der Pharmacia Lettre. 2012; 4: 1272-84.

Sofowora A. Research on medicinal plants and traditional medicine in Africa. J Altern Complem Med. 1996; 2: 365-72.

Ullah R, Hussain Z, Iqbal Z, Hussain J, Khan FU, Khan N, Muhammad Z, Ayaz S, Ahmad S, Rehman NU. Traditional uses of medicinal plants in Darra Adam Khel NWFP Pakistan. J Med Plant Res. 2010; 17: 1815-21.

Yim T, Wu W, Pak W, Ko K. Hepatoprotective action of an oleanolic acid-enriched extract of *Ligustrum lucidum* fruits is mediated through an enhancement on hepatic glutathione regeneration capacity in mice. Phytother Res. 2001; 15: 589-92.

Yue J, Peng R-X, Yang J, Kong R, Liu J. CYP2E1 mediated isoniazid-induced hepatotoxicity in rats. Acta Pharmacol Sin. 2004; 25: 699-704.

Supplementary

Compound 1 (oleanolic acid)

Compound 1 (Figure 2) was isolated from the subfraction "A" of ethyl acetate fraction of hydro-ethanolic (3:7) extract of *M. buxifolia* fruit. Compound was purified through repeated column chromatography using normal phase silica gel as stationary phase. Mobile phase used were ethyl acetate : hexane (1:9).

Structure elucidation

Compound 1 was isolated from the ethyl acetate fraction through normal phase column chromatography. The EI-MS

(Calc. 456.6840) (Supplementary Table I). The mole-cular formula indicated seven degrees of un-saturation. Six degrees of un-saturation indicated the presence of six double bonds, while remaining one corresponded to the presence of a double bond in compound **1**.

The ^{1}H-NMR (MeOD 300 MHz) spectrum of compound **1** showed an olefinic H-12 one proton integration as a broad triplet at δ 5.22 (Supplementary Table II). The OH-substituted methine (CH-3) appeared as a double doublet at δ 3.17 (1H, dd, $J_{3, 2a}$ = 5.1 Hz, $J_{3, 2β}$ = 10.8 Hz). The H-18 showed a signal at δ 2.21 (1H, dd, $J_{18, 19a}$ = 11.1 Hz, $J_{18, 19β}$ = 16.1 Hz). Seven methyl groups appeared in the ^{1}H-NMR spectrum of compound **6**. The germinal CH$_3$-23 and CH$_3$-24 appeared at δ 0.98 and 0.95 (3H, s) respectively. Similarly CH$_3$-25, CH$_3$-26 and CH$_3$-27 appeared as singlets at δ 0.98, 0.94 and 1.15, respectively. The CH$_3$ -29 and CH$_3$-30 also appeared as a singlet at δ 0.80 and 0.77, respectively.

Compound 2 (isoquercetin)

Compound **2** was purified from the sub-fraction "M" of ethyl acetate fraction. The sub-fraction was re-chromatographed using normal phase silica gel as stationary phase. Compound **2** purification was made possible using solvent systems ethyl acetate : hexane (8:2).

Structure elucidation

Compound **2** was isolated from the ethyl acetate fraction using

repeated column chromatography. The FAB (-ve) of compound **2** showed pseudo-molecular ion peak [M-H] at *m/z* at 463. The HRFAB-MS (-ve) indicated the molecular formula at $C_{21}H_{20}O_{12}$ at *m/z* 463.0012. The IR (KBr) shows absorption characteristic for flavonoids appeared at 3415 (OH), 1650, 1433 Cm^{-1} (due to double bonds of aromatic rings). The C-H stretching appeared at 2918 while C-O appeared at 1056 Cm^{-1}. The UV (MeOH) shows absorption signal at 213, 260 and 360 nm indicated the conjugated system in compound.

The ^{1}H-NMR (MeOD, 300 MHz) showed a meta coupled doublet appeared at δ 7.84 (1H, d, $J_{2', 6'}$ = 2.1 Hz, H-2') (Supplementary Table III). Similarly the H-6' showed a meta coupling with H-2' appeared at δ 7.59 (1H, d, $J_{6'2'}$ = 2.1 Hz). The H-3' appeared at δ 6.87 (1H, d, $J_{3'2'}$ = 8.4 Hz) which showed an artho coupling with H-2' of aromatic ring B. The H-8 of ring A appeared at δ 6.87 (1H, d, $J_{8, 6}$=1.8 Hz). Similarly the H-6 of ring A appeared at δ 6.20 (1H, d, $J_{8, 6}$ = 2.1 Hz). From the J value it shows that both are meta coupled to each other. The glucose moiety with ring C of compound 2 shows the anomeric proton appeared at δ 5.17 (1H, d, $J_{1'', 2''}$=7.5 Hz). The H-2'' of glucose appeared at δ 3.84 (1H, d, J2'', 1''=2.4/J2'', 3'' = 1.8 Hz). The H-3'' appeared at δ 3.78 (1H, brs). The H-4'' appeared at δ 3.67 (1H, dd, J4'') The H-5'' exhibited at 3.5 (1H,m) The H-6'' methylene proton appeared at δ 3.54 (2H,m)

The ^{13} C-NMR (BB and DEPT) showed a total of 21 carbon atoms. Among which 10 are quaternary and 10 are methine (CH) carbon atom which the dept 135 shows the presene of
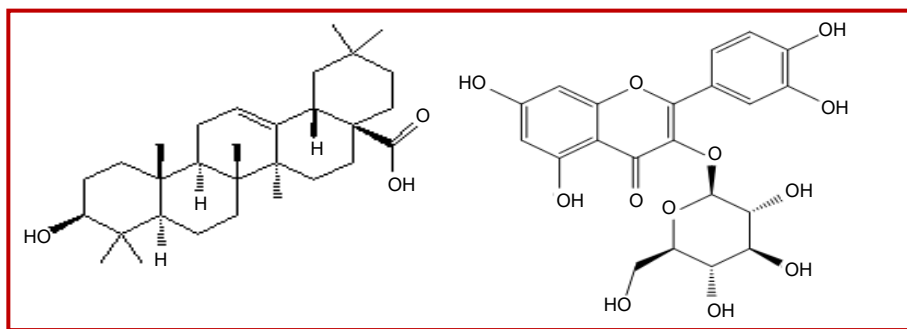

Figure 2: Structure of compound 1 (oleanolic acid, left) and compound 2 (isoquercetin, right)

Supplementary Table I		
Characteristics of compounds		
Parameters	Oleanolic acid	Isoquercetin
Physical state	White amorphous powder	Yellow amorphous powder
Molecular formula	$C_{30}H_{48}O_3$	$C_{21}H_{20}O_{12}$
$[α]^{26}{}_D$		-76
Melting point		245°C
UV activity	Inactive on UV	UV active on TLC
R*f*. Value	0.43 ethyl acetate : hexane (2:8)	
Yield	40 mg	30.5 mg
Solubility	DCM (room temperature)	Methanol, DMSO
UV l$_{max}$ ()		213, 260 and 360 nm
IR spectrum cm^{-1}		3415 (hydroxyl), 1650, 1433 (double bonds of aromatic rings)
HREI-MS	456.7003 (Calc. 456.6840)	463.0012 [M-H]

Supplementary Table II			
¹³C- and ¹H-NMR chemical shift values of compound 1			
Carbon	δ_H (J, Hz)	Multiplicity	δ_C
1	1.57, 1.32	CH_2	38.1
2	1.73, 1.46	CH_2	27.9
3	3.16 (1H, dd, $J_{3,2a}$ = 4.8 Hz / $J_{3,2\beta}$ = 2.0 Hz)	CH	79.7
4	–	C	39.8
5	1.39 (1H, m)	CH	56.8
6	1.54, 1.27 (2H, m)	CH_2	19.5
7	1.57, 1.36 (2H, m)	CH_2	33.9
8	–	C	42.7
9	1.43 (1H, m)	CH	47.3
10	–	C	38.1
11	2.04, 1.79 (2H, m)	C	23.9
12	5.24 (1H, t, $J_{12,11}$ = 6.5 Hz)	CH	123.6
13	–	C	145.2
14	–	C	42.8
15	1.34, 1.03 (2H, m)	CH_2	28.9
16	1.71, 1.18 (2H, m)	CH_2	24.5
17	–	C	47.7
18	2.16 (1H, dd, $J_{3,2a}$ = 4.8 Hz, $J_{3,2\beta}$ = 2.0 Hz).	CH	42.9
19	1.51, 1.45 (2H, m)	CH_2	46.3
20	–	C	30.7
21	1.61, 1.35 (2H, m)	CH_2	34.9
22	1.72, 1.48 (2H, m)	CH_2	33.0
23	0.94 (3H, s)	CH_3	23.9
24	0.93 (3H, s)	CH_3	23.9
25	0.97 (3H, s)	CH_3	15.9
26	0.90 (3H, s)	CH_3	16.3
27	1.15 (3H, s)	CH_3	26.4
28	––	CH_3	24.5
29	0.77 (3H, s)	CH_3	24.1
30	0.80 (3H, s)	C	181.8

MeOD, ppm, 125 and 500 MHZ respectively

Supplementary Table III		
¹³C- and ¹H-NMR chemical shift values of compound 2		
Carbon	δ_H (J, Hz)	δ_C
1	–	–
2		158.4
3		138.7
4	–	178.9
5	–	166.2
6	6.20 (1H, d, $J_{6,8}$ = 2.1 Hz)	99.9
7	–	163.0
8	6.87 (1H, d, J8, 6=1.8 Hz)	94.7
9	–	158.8
10	–	105.6
1'	–	122.5
2'	7.84 (1H, d, $J_{2', 6'}$, 2.1)	122.9
3'	6.87 (1H, d, $J_{3'2'}$ = 8.4 Hz)	117.8
4'	–	149.0
5'	–	145.8
'6	7.59 (1H, d, $J_{6'2'}$ = 2.1 Hz)	116.1
1''	5.17 (1H, d, $J_{1'', 2'}$ =7.5 Hz).	105.4
2''	3.84 (1H, d, $J_{2'', 1'}$, $J_{2'', 3''}$ = 2.4, 1.8 Hz	75.1
3''	3.78 (1H, brs	73.2
4''	3.67 (1H, dd, $J_{4'',3''}$=---Hz/J4'', 5''=---Hz	70.0
5''	3.5 (1H,m)	77.1
6''	3.54 (2H,m)	61.9
MeOD, ppm, 125 and 500 MHZ respectively		
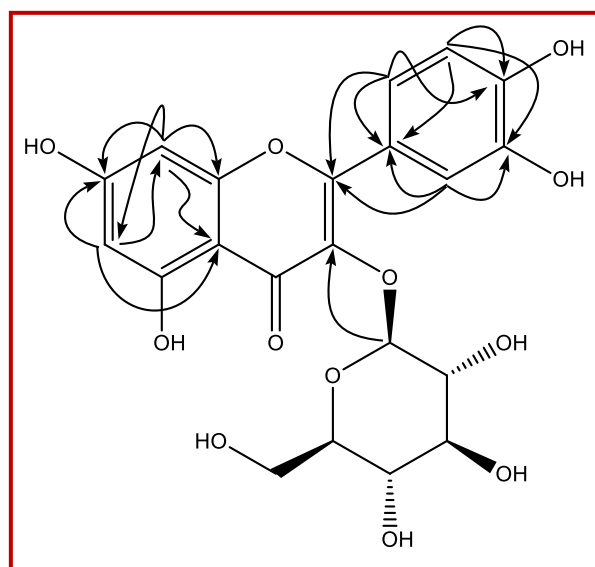
Figure 3: Key COSY and HMBC structure of isoquercetin

one methylene. The OH substituted carbon atom of aromatic ring A appeared at δ 166.2 and 163.0 for C-5 and C-7. The OH bearing carbon atom of ring B appeared at δ 149.0 and 145.8 for C-4 and C-5.

The quaternary carbon atom C-9 and C-10 appeared at δ 158.8 and 105.6. The ring C quaternary carbon atoms appeared at δ 158.4 and 135.7 for C-2 and C-3. The C-6 and C-8 methine (CH) carbon atoms of compound exhibited at δ 99.9 and 94.7. The methines of aromatic ring B at C-2' and C-6' appeared at δ 122.9 and 116.1. The compound **9** also contains a glucose

moiety the anomeric carbon atom C-1 appeared at δ 105.4. The OH- substituted carbon atoms C-2″, C-3″, C-4″ appeared at δ 75.1, 73.2 and 70.0 respectively. The methine C-5″ of compound **2** appeared at δ 77.1. The methylene C-6″ of glucose moiety of compound **2** appeared at δ 61.9. The α/β unsaturated carbon atoms of ring C appeared at δ 179.5

The H-2′ shows HMBC connectivity with C-1′, C-4′ and C-5′ of aromatic ring B (Figure 3). the H-2′ also connected to C-2 of pyran ring C though HMBC correlation. The H-6′ shows correlation with C-2′ and C-5′ of aromatic ring B, while it also shows connection to C-2 of ring C. The H-3′ shows connectivity to C-1′, C-4′, C-5′ and C-6′ of ring B. the H-8 of ring A gives its connection through HMBC correlation with C-4 carbonyl, C-9 and C-10 quaternary carbon and C-7 OH substituted carbon and C-6 methine carbon atom. The position of H-6 confirmed through HMBC correlation by its connectivity to the adjacent carbon atoms (C-8, C-10, C-5 and C-7). The anomeric proton of glucose moiety shows connectivity to C-2″ and C-3carbon atom. So, from HMBC it was confirmed that the glucose moiety attached to C-3 of ring C which shows HMBC correlation between anomeric protons of glucose to C-3 at 136.0

Author Info
Jamshaid Ali Khan (Principal contact)
e-mail: jamshaidkhan@upesh.edu.pk